Title

Low-dose polylactic acid microplastics mitigate methane emissions in ratoon rice systems

Sha Zhang[a,b,1]*, Qianrui Huangfu[c,1], Lu Wang[a,b], Zheng Chen[d]*, Dong Zhu[a,b]*

[a] State Key Laboratory of Regional and Urban Ecology, Ningbo Observation and Research Station, Institute of Urban Environment, Chinese Academy of Sciences, Xiamen 361021, China

[b] Zhejiang Key Laboratory of Urban Environmental Processes and Pollution Control, Chinese Academy of Sciences Haixi Industrial Technology Innovation Center in Beilun, Ningbo 315830, China

[c] Department of Chemical and Environmental Engineering, University of Nottingham-Ningbo China, Ningbo 315100, China

[d] Department of Health and Environmental Sciences, Xi'an Jiaotong-Liverpool University, 111 Ren'ai Road, Suzhou, Jiangsu, 215123, China

[1] The authors contributed equally.

*Corresponding authors

Primary contact:

Sha Zhang

Assistant Research Professor

https://orcid.org/0000-0002-8080-5073

Tel: +86-17798590069

Email: biogeochemx@outlook.com, szhang@iue.ac.cn

Address: Ningbo Observation and Research Station

Institute of Urban Environment, Chinese Academy of Sciences

No. 88 Zhongke Road, Chunxiao Street

Beilun District, Ningbo City

Zhejiang Province, China

Postal Code: 315800

Graphical Abstract

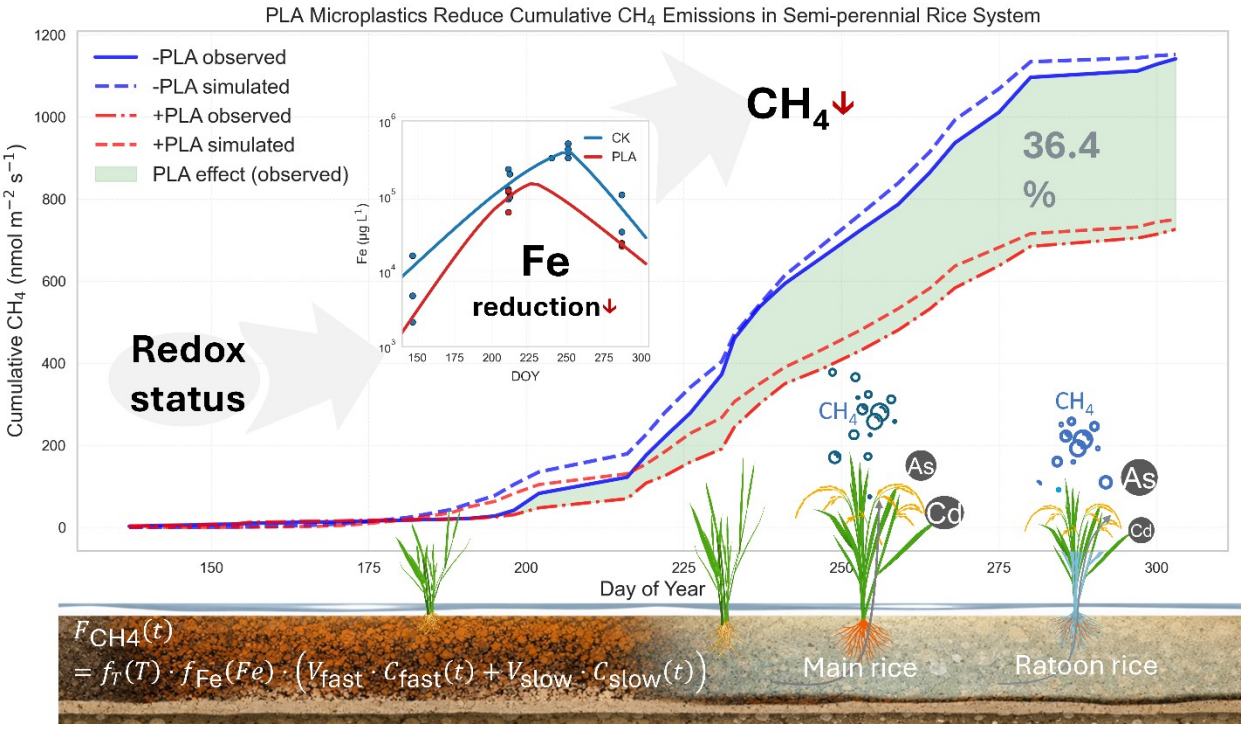

Abstract

Biodegradable plastics are increasingly introduced into agricultural systems, yet their ecosystem-scale climate impacts on methane (CH_4) emissions remain poorly understood. Here, we evaluated the effects of environmentally realistic, low-dose polylactic acid (PLA) microplastics on CH_4 emissions and food safety across a full ratoon rice growing cycle. PLA amendment reduced cumulative methane (CH_4) emissions by 36.4% (8.42 ± 0.54 vs. 5.35 ± 0.27 g m^{-2}) without affecting CO_2 exchange, crop productivity, or grain metal(loid) concentrations. Temporal analyses revealed that CH_4 dynamics were primarily governed by crop phenology. Process-based modeling evidence indicated that PLA induced persistent soil redox regulation, suppressing methanogenesis while avoiding the typical trade-off between CH_4 mitigations and heavy-metal risks. Moreover, PLA reduced the apparent temperature sensitivity of CH_4 emissions, suggesting enhanced system stability under heat extremes. These findings identify a previously overlooked pathway linking biodegradable material inputs with ecosystem CH_4 regulation and highlight their potential contribution to carbon-neutral agricultural management.

Keywords

PLA microplastics; methane emissions; ratoon rice; soil redox; biodegradable plastics; carbon neutrality

Highlights

- Environmentally realistic PLA microplastics reduced seasonal CH_4 emissions by 36.4%.
- Methane mitigation occurred without yield penalty or grain metal accumulation.
- Soil redox regulation, rather than temperature sensitivity, governed CH_4 dynamics.
- PLA decoupled greenhouse gas mitigation from food-safety trade-offs.
- PLA exhibit unexpected climate-regulation functions in agroecosystems.

Introduction

Rice paddies contribute approximately 8–12% of global anthropogenic methane (CH_4) emissions [1]. Emission rates are highly sensitive to subtle shifts in carbon availability, soil redox conditions, and plant-mediated gas transport, rendering flooded rice systems highly responsive to environmental perturbations [2]. Meanwhile, agricultural soils are increasingly exposed to microplastics through mulching residues, irrigation inputs, and polymer-containing amendments [3]. Biodegradable plastics, particularly polylactic acid (PLA), are widely promoted as environmentally sustainable alternatives to conventional polymers. Although PLA can theoretically undergo anaerobic mineralization to CH_4 under thermophilic conditions [4-9], its degradation under mesophilic paddy conditions (typically below ~30 °C) is extremely slow (e.g., 0.065 mg day^{-1} ref[10]), often persisting for years, decades, or even centuries [6, 8, 9]. Consequently, PLA residues are more likely to interact with soil biogeochemical processes than to serve as direct CH_4 substrates during crop growth periods [6]. Despite this, the effects of environmentally relevant PLA inputs on CH_4 emissions under realistic rice cultivation scenarios remain unreported [11-14].

Emerging evidence indicates that PLA plastics can influence microbial metabolism and soil redox dynamics [8-10, 15, 16]. However, the reported effects of PLA on CH_4 emissions are inconsistent, with both stimulatory and inhibitory outcomes documented [17]. These discrepancies likely arise from experimental limitations, as many investigations rely on plant-free incubations, short-term pot experiments, or incomplete seasonal observations [18, 19]. These approaches fail to capture the coupled soil–plant continuum regulating CH_4 emissions in rice ecosystems, where plant aerenchyma transport and rhizosphere-driven redox oscillations strongly shape CH_4 production and release [18, 19].

Against this backdrop, the effects of environmentally realistic, low-dose PLA inputs on CH_4 emissions under field-relevant, full-season crop conditions remain virtually unexplored. Beyond serving as physical residues, PLA particles introduce abundant oxygen-containing

functional groups and reactive surfaces to soil components [14, 20, 21], potentially modulating microbial electron transfer processes [14, 15]. One mechanism potentially involves competition among terminal electron-accepting processes. Within flooded soils, Fe(III) reduction thermodynamically precedes methanogenesis and can consume up to 50% of available electron donors, suggesting that variations in reactive Fe cycling may serve as a redox proxy for CH_4 flux dynamics [15, 22-24]. Detecting low-dose effects typically requires extended observation periods. Whether PLA microplastics modulate these competing pathways under field-relevant crop growth conditions remains unresolved [18, 25]. This knowledge gap is particularly pronounced in long-growth systems such as semi-perennial (ratoon) rice, where sustained plant activity fundamentally modifies carbon allocation and seasonal CH_4 emission patterns [26].

By integrating gas flux measurements, soil–water chemistry, and plant responses under field-relevant conditions, this study tests the hypothesis that environmentally realistic PLA microplastic inputs (0.01% w/w) regulate CH_4 emissions through persistent soil redox modulation. We further examine whether such regulation alters the apparent temperature sensitivity of CH_4 emissions and alleviates the commonly observed trade-off between greenhouse gas mitigation and grain food safety. Clarifying these mechanisms provides a process-based framework for evaluating biodegradable materials not only as emerging soil residues but also as potential modifiers of ecosystem-scale carbon dynamics in agricultural systems.

2. Materials and Methods

2.1. Soil location and characterization

Paddy soil was collected from Qingyuan city (23.35N, 113.33E), Guangdong province of China, characterized by total soil organic carbon (SOC, 1.4%) and total nitrogen (0.09%), with a pH of 5.6. The soil contains 12% iron (Fe), 50.7 g kg^{-1} As, and 0.2 mg kg^{-1} Cd.

2.2. PLA characterization

EN 13432:2000 mandates that compostable polymers achieve ≥90% mineralization to CO_2 within 6 months under aerobic conditions. For anaerobic conditions, it requires ≥50% conversion to biogas (relative to theoretical maximum) within 2 months [27]. This time scale match with rice growth duration. Ingeo™ Biopolymer 4032D PLA (NatureWorks, the United States) powder (25 μm) was used and met the EN 13432:2000 standard. The powder is turbid and opaque, suggesting a lower molecular weight (e.g., Mw <100,000 D) and better biodegradability [28].

2.3. Open-field rice growth experiment

A field pot experiment assessed PLA microplastic impacts on greenhouse gas emissions throughout the ratoon rice growth cycle. Treatments comprised unamended (−PLA) and PLA-amended (+PLA) rice, each replicated three times in individual pots. Basal N fertilizer (urea, 60 kg N ha^{-1} equivalent for 6 kg soil) was applied at planting. Yliangyou No.1 rice seedlings were germinated in deionized water, grown 4 weeks on horticultural substrate, then transplanted as single hills (3–4 plants, 25 days old) per pot. Pots were positioned within a flooded sand bed (river sand volume ≥5× total pot volume) maintaining ~5 cm standing water above soil. Rainfall collection supplemented irrigation to offset evaporation and sustain continuous flooding. Soil temperature at 5–10 cm depth was logged every 30 min via thermocouples linked to a data logger (Xiandun CIMC Inc., China) [26].

2.4. Chamber-based CH_4 flux measurement

Methane and CO_2 fluxes were quantified every 3–10 days using static chambers (V = 0.1925 m^3, A = 0.12 m^2) connected to a LI-7810 analyzer (LI-COR), calculating rates from initial linear concentration increases 30 s post-closure via Eq. 1.

Where J is flux (μmol m^{-2} s^{-1}); P = 101.3 kPa; R = 0.008134 m^3 kPa mol^{-1} K^{-1}; T = soil temperature (5 cm); W_0 = mean H_2O mole fraction; ∂C/∂t from linear regression (R^2 > 0.75, RMSE < 2 ppb CH_4 or 1.5% CO_2). Half-transparent chambers captured NEE under ambient light. The analyzer was auto-calibrated with standards; disturbed measurements (ebullition, perturbations) were rejected. Concurrent records included soil temperature (5 cm), air temperature, RH, and PPFD from a micro-weather station. More details were described elsewhere [29, 30].

2.5. Soil microdialysis and dissolved Fe analysis

Following the practices in Huangfu et al. [31, 32], rhizosphere porewater was sampled via in situ microdialysis probes (~10 cm depth) throughout the experiment, intensified during key rice growth stages, to track root-zone redox dynamics, with dialysate collected in acid-cleaned vials (pH < 2, HNO_3) for ICP-MS Fe analysis (calibrated with standards, RSD < 5%). Dissolved Fe and other redox-sensitive elements (i.e., Thallium, Tl; Manganese, Mn; Copper, Cu; Selenium, Se and As) served as a redox proxy rather than direct Eh values; their temporal patterns, integrated with CH_4/CO_2 fluxes, revealed PLA-driven rhizosphere redox shifts controlling CH_4 emissions in ratoon rice.

2.6. Process-based CH_4 modeling

2.6.1. Conceptual framework

We developed a process-based model to simulate CH_4 emissions from flooded rice paddies by coupling dynamic carbon inputs, temperature effects, and Fe-mediated redox competition. The model explicitly represents two reducible soil carbon pools: a fast-decaying pool () and a slow-decaying pool (), which together constitute the active substrate available for methanogenesis. Carbon inputs originate from root exudates, rice litter, and soil organic matter, and are partitioned into the two pools according to a variable fraction. To account for delayed carbon translocation to the soil, particularly under PLA microplastic treatments, a lag parameter shifts the temporal availability of carbon to microbial

communities. Methane emissions arise mainly from both plant- and soil-derived carbon processed by anaerobic microbes [19]. CH_4 fluxes arise from plant- and soil-derived carbon processed by anaerobic microbes. The model ensures mass conservation and mechanistic interpretability by explicitly linking parameters to identifiable ecological processes. Key constraints include: (1) Substrate limitation that only the and pools are available for CH_4 production; (2) Temperature control that microbial kinetics follow a Gaussian response function approximating the temperature sensitivity of methanogenesis; and (3) Redox gating that Fe(III) reduction competitively consumes electron donors, delaying CH_4 release until Fe(III) becomes limiting.

2.6.2. Reducible carbon pool dynamics

Temporal dynamics of the carbon pools are modeled as Eqs 2—3.

where is the slow fraction, and and are decay constants controlling microbial accessibility. To represent delayed carbon availability, particularly in +PLA treatments, the carbon pools are shifted forward in time by a lag parameter. Carbon input is calculated from photosynthetic activity as Eq. 4.

with and representing the fractions of gross primary production allocated directly and indirectly (via turnover) to the soil carbon pools.

2.6.3. Temperature and Fe regulation

Microbial CH_4 production is modulated by temperature and Fe availability (Eqs 5—6). A Gaussian function describes the sensitivity of methanogenesis to soil temperature (T)

meanwhile Fe availability inhibits CH_4 production according to a Michaelis-Menten relationship.

Where is the optimal temperature and controls the width of the temperature response. is the dissolved Fe concentration. is the half-saturation constant. This formulation captures the competitive consumption of electron donors by Fe(III) reduction and its indirect suppression of methanogenesis.

2.6.4. CH_4 emission equation

Simulated CH_4 flux is calculated as Eq. 7.

Where and are maximum CH_4 production capacities for the fast and slow pools. The lagged carbon input dynamically parameterizes and to capture the temporal dependence of substrate supply on CH_4 fluxes.

2.6.5. Model parameters and input variables

All parameters correspond to measurable ecological processes and are calibrated against observed CH_4 fluxes. Key parameters and ranges are summarized in Table 1. Input variables include time-resolved soil temperature (°C), total dissolved Fe (i.e., proxy for Fe^{2+}, mg L^{-1}) in the root zone, and net CO_2 flux as a proxy for photosynthetic carbon supply (μmol m^{-2} s^{-1}).

198 **Table 1.** Model parameters, symbols, physical meaning, and typical ranges.

Parameter	Symbol	Unit	Ecological meaning	Typical range
Maximum CH_4 capacity – fast pool		μmol m^{-2} s^{-1}	Maximum CH_4 production potential for the fast carbon pool under optimal redox and temperature	1–100 [33]
Maximum CH_4 capacity – slow pool		μmol m^{-2} s^{-1}	Maximum CH_4 production potential for the slow carbon pool	1–50
Fe half-saturation		mg L^{-1}	Fe^{2+} concentration that half-suppresses CH_4 production	10–700 [34]
Fast carbon decay rate		d^{-1}	Fraction of fast carbon pool decayed per day	0.01–0.3 [9]
Slow carbon decay rate		d^{-1}	Fraction of slow carbon pool decayed per day	0.001–0.1 [9, 10]
Temperature optimum		°C	Temperature at which microbial CH_4 production is maximal	20–35 [9, 35]
Temperature response width		°C	Width of the Gaussian temperature response	4–12 [36]
Root allocation fraction		–	Fraction of GPP directly allocated to roots and soil	0.3–0.4 [37]
Turnover allocation fraction		–	Fraction of dip/dt contributing to soil carbon input	0.2–0.3 [38]
Carbon lag effect		d	Temporal shift of carbon availability due to PLA disturbance	0–15 [9]

199 **2.6.6. PLA disturbance representation**

PLA microplastics are modeled as an **indirect disturbance**, altering soil reactive surface areas and microbial habitats. Their effects are implemented by: (1) Introducing a temporal lag in carbon availability to the pools (lag parameter); (2) Modifying carbon input fractions and fitted CH_4 production parameters (+PLA vs −PLA treatments). No additional substrate is added. Comparative parameter inversion between +PLA and −PLA treatments enables mechanistic inference of how PLA influences CH_4 fluxes at the system scale.

2.7. Statistical analysis

Analyses used Python 3.10 (`numpy`, `pandas`, `scipy`, `statsmodels`). Means ± SD reported. Treatment effects on stage-averaged fluxes/chemistry tested by two-tailed t-tests (`α = 0.05`; Shapiro-Wilk normality, Levene's homogeneity verified). Pseudoreplication avoided via stage-means (n=3). Effect sizes: Cohen's d. Fold-changes quantified relative differences. CH_4-environment regressions used OLS (`statsmodels`; R^2, $p<0.05$, Durbin-Watson autocorrelation test). Residual diagnostics (normality, homoscedasticity) confirmed model validity. Outliers (|z|>3 SD) excluded; missing data listwise deleted.

3. Results

3.1. Seasonal CH_4 and CO_2 fluxes

Over the 167-day full life cycle, 0.01% (by w.t.) PLA markedly reduced cumulative CH_4 emissions by 36.4% from 8418 ± 538 mg m^{-2} to 5354 ± 270 mg m^{-2}. No detectable PLA effects were observed during the first 40 days (DOY 135–175) after transplanting (Fig. 1a, inset); thereafter, CH_4 fluxes were consistently lower for the remainder of the rice growth period. In contrast, mean CO_2 fluxes showed only minor differences between treatments. Although PLA did not alter the overall seasonal pattern of CH_4 fluxes, the treatment effect emerged in the context of natural temporal variability. Methane emissions increased rapidly during the tillering and jointing stages, declined during grain filling, and remained elevated through the ratoon season (Fig. 1a). Following transplanting, CH_4 fluxes remained low (0–4 nmol m^{-2} s^{-1}) for ~25 days in both groups, despite steadily increasing air and soil

226 temperatures within ranges favorable for microbial activity. A transient heatwave (DOY
227 187–193), during which daily maximum air temperatures exceeded 35 °C for three
228 consecutive days, did not trigger an increase in CH_4 emissions in either treatment,
229 demonstrating that the PLA effect was robust to short-term temperature extremes.
230 Divergence between treatments became evident after ~25 days post-transplanting, when
231 +PLA consistently suppressed CH_4 fluxes relative to −PLA.

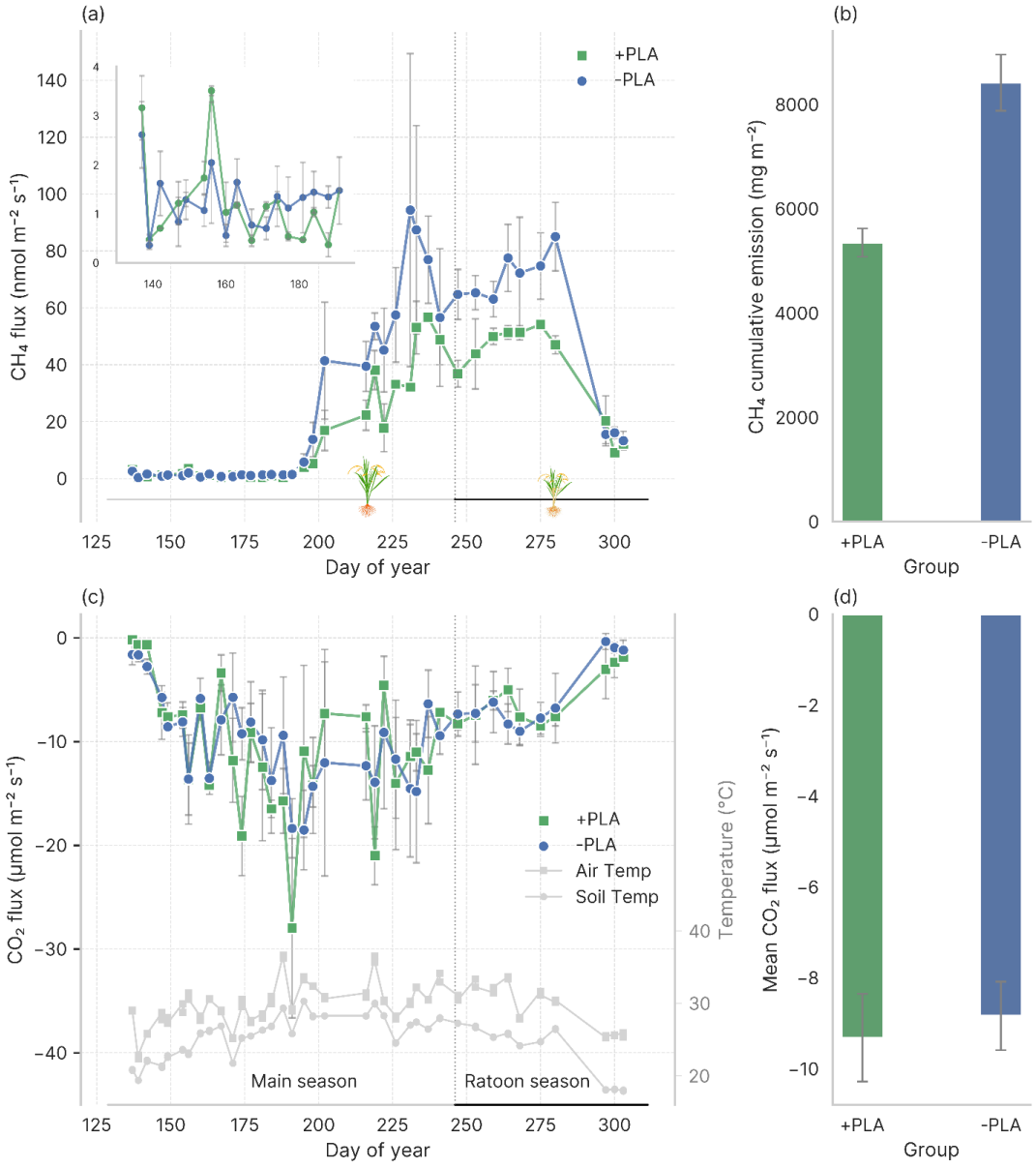

232

Fig. 1. Methane and CO_2 fluxes and temperature dynamics in ratoon rice system with (+PLA) and without (-PLA) plastic addition. (a) Temporal dynamics of CH_4 flux (nmol m^{-2} s^{-1}). The inset shows details during the seedling stage of main crop rice. (b) Cumulative CH_4 emissions (mg m^{-2}) calculated by temporal integration. (c) Temporal dynamics of CO_2 flux (μmol m^{-2} s^{-1}) with air (triangle) and soil (circle) temperatures (°C). (d) Mean CO_2 flux (μmol m^{-2} s^{-1}) across the measurement period. The dashed vertical line at day of year 246 marks the transition between main and ratoon seasons. Data are shown as means ± SD (n = 2-3).

Regression analyses indicated that the PLA-driven variation in CH_4 fluxes was indirectly influenced by environmental conditions. Among all measured variables, air temperature showed a modest positive relationship with CH_4 fluxes, accounting for roughly 15% of the observed variability, whereas soil temperature, RH, VPD, and PPFD had weak or non-significant effects (Table S1). Although contemporaneous CO_2 and CH_4 fluxes were poorly correlated, a significant correlation emerged when CO_2 fluxes were lagged by 5 days (−PLA R^2 = 0.318; +PLA R^2 = 0.286; Fig. 1a,c; Fig. S1). CO_2 fluxes themselves were closely related to both air and soil temperatures (Fig. S2). Taken together, these patterns indicate that temperature effects on CH_4 fluxes may operate indirectly through temporally delayed changes in CO_2 fluxes, even though direct correlations are weak.

3.2. Soil redox dynamics

The “redox ladder” presented in Fig. 2a provides a thermodynamic framework for contextualizing the selection of these elements as indicators spanning a range of redox sensitivities. Collectively, +PLA soils showed a higher oxidation status as indicated by a lower dissolved Mn, As and Fe concentrations (Fig. 2c, f, g; Fig. 3). The time-series profiles in Fig. 2b–g highlight a divergence in how individual redox-sensitive elements respond to PLA amendment, with several elements exhibiting attenuated temporal dynamics relative to the -PLA series during the tillering stage (DOY 211–212). Across the sampling period

encompassing the flowering stage of the first rice season, distinct element-specific response patterns emerged between treatments. In the −PLA control, dissolved concentrations of Tl, Mn, As, and Fe exhibited pronounced short-term fluctuations, characterized by clear diel-scale variability across consecutive sampling points (Fig. 2b–e). In contrast, under +PLA conditions, the temporal variability of these elements became markedly dampened, with concentration profiles displaying reduced amplitude and weakened day–night contrasts. By comparison, Cu and Se showed a different response pattern. For both elements, temporal trends under +PLA largely followed those observed in the −PLA control, including comparable short-term variability and directional changes over the sampling sequence (Fig. 2f–g). The overall concentration ranges and temporal trajectories of Cu and Se remained similar between treatments. Across both the main and ratoon cropping seasons, +PLA consistently showed lower porewater Fe and As concentrations (Fig. S3, S4). Two-way ANOVA indicates that these treatment differences are statistically significant for Fe ($p = 0.009$) and As ($p = 0.002$), while other redox-sensitive elements (Mn, Tl) did not show significant changes.

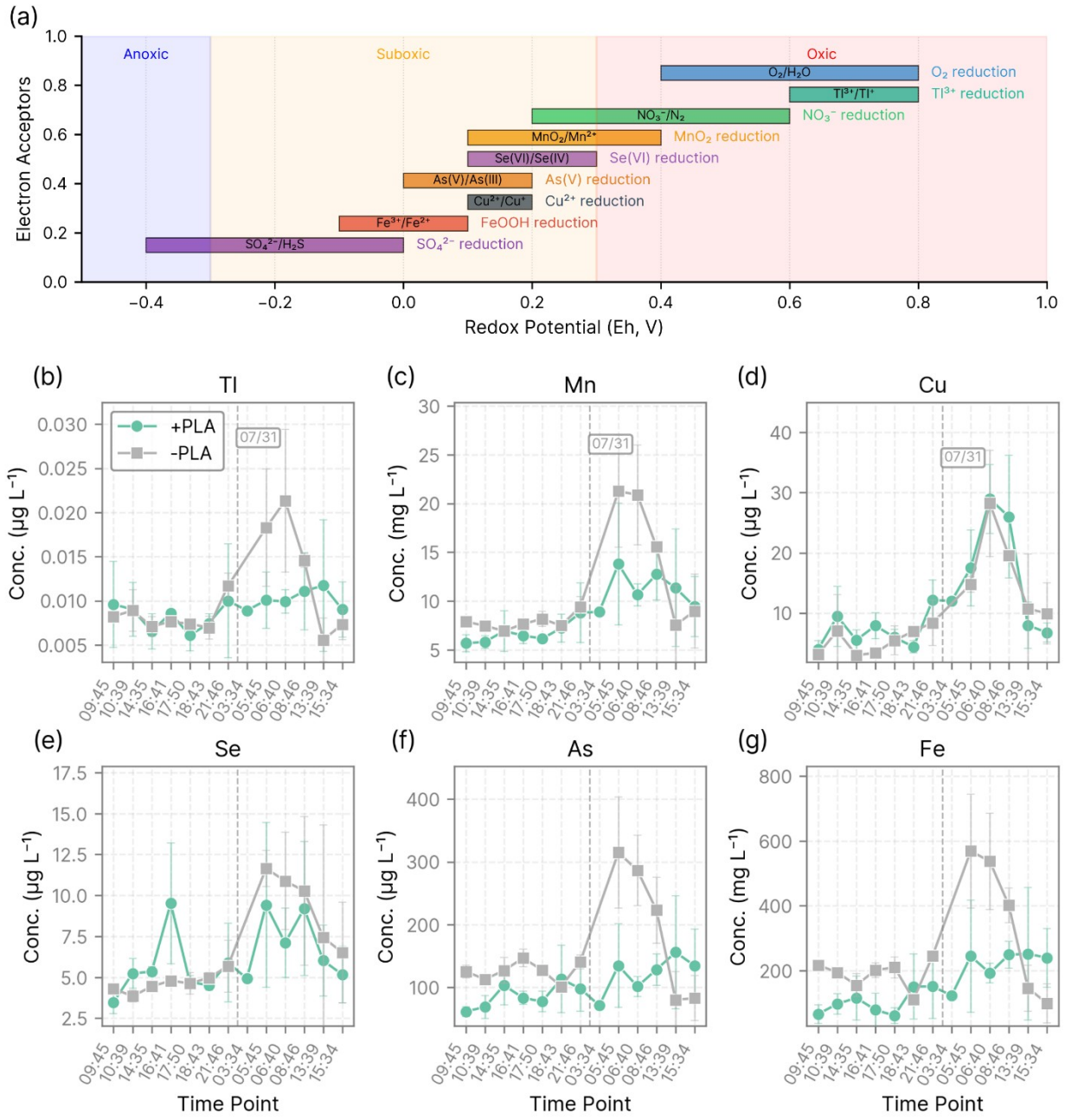

275

276 **Fig. 2. Redox framework and time-resolved dynamics of dissolved porewater**
277 **constituents during the experimental period. (a)** Conceptual redox ladder illustrating
278 the typical ranges of redox potential (Eh) associated with dominant terminal electron-
279 accepting processes in flooded soil–water systems, including oxygen, nitrate, metal(loid)
280 oxides (Mn, Fe, As, Tl, Cu, Se), and sulfate reduction. Colored horizontal bars indicate
281 approximate Eh windows under which each reduction pathway is thermodynamically

favored, with representative redox couples shown within each bar. Shaded background zones denote oxic, suboxic, and anoxic conditions. **(b–g)** Temporal variations in dissolved porewater concentrations of representative redox-sensitive elements measured at sequential sampling points under different treatment groups. Data are presented as mean ± standard deviation (n = 3).

3.3. Model simulations

Model simulations demonstrated that the CH_4 model integrating dual carbon pools, an Fe redox indicator, and a Gaussian temperature response reproduced observed CH_4 flux dynamics across −PLA and +PLA treatments (Fig. 3). The model showed strong predictive performance under both treatments, explaining 90.9% of the variance in observed CH_4 fluxes in the −PLA treatment (R^2 = 0.909, RMSE = 9.83 nmol m^{-2} s^{-1}, n = 38) and 87.1% in the +PLA treatment (R^2 = 0.871, RMSE = 7.41 nmol m^{-2} s^{-1}, n = 38; Fig. 3b). Seasonal cumulative CH_4 emissions derived from model simulations closely reproduced treatment-level emission differences, with a deviation of 1.1% between simulated and observed reductions (Fig. 3c). Minor systematic deviations were observed, with slight underestimation at low fluxes and overestimation near peak emission periods.

Parameter estimation revealed treatment-specific differences in simulated CH_4 production dynamics (Fig. 3d). In the −PLA treatment, CH_4 production involved contributions from both fast and slow carbon pools, with fitted maximum production rates of = 2.92 ± 9.53 and = 1.33 ± 4.35, respectively, where uncertainties (±) denote asymptotic standard errors derived from the covariance matrix of the nonlinear least squares optimization. Under the +PLA treatment, the fitted contribution of the fast carbon pathway approached zero (≈ 0±7.75), whereas CH_4 production was primarily associated with the slow carbon pool (= 1.69 ± 1.98). The estimated Fe half-saturation constant decreased from 110.23 ± 106.84 mg kg^{-1} in −PLA soils to 54.26 ± 51.50 mg kg^{-1} in +PLA soils, indicating increased Fe sensitivity of CH_4 production under PLA exposure. Temperature response parameters ()

also differed between treatments, with fitted optimum temperature and response width varying between model realizations. Parameter uncertainties were comparatively large across several coefficients, reflecting partial parameter compensation and equifinality typical of nonlinear process-based biogeochemical models. Despite uncertainty in individual parameters, simulated CH_4 flux trajectories and cumulative emissions remained consistently constrained across treatments, indicating that treatment-dependent responses emerged robustly at the system level rather than relying on unique parameter combinations.

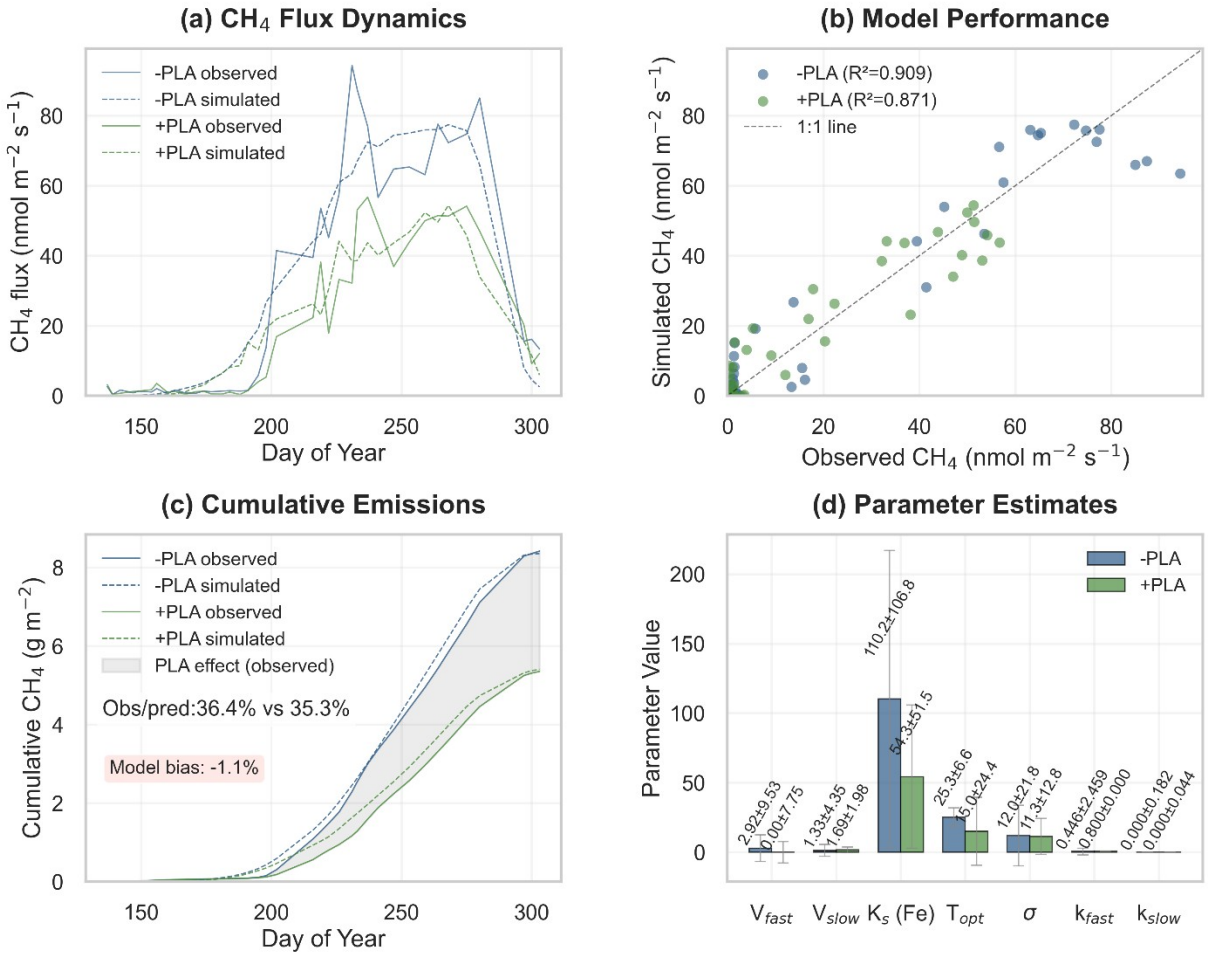

Fig. 3. Model evaluation and parameter estimation of CH_4 dynamics under −PLA and +PLA treatments.

(a) Seasonal dynamics of observed and simulated CH_4 fluxes using the improved CH_4 model integrating dual carbon pools, Fe limitation, and Gaussian temperature response. (b) Relationship between observed and predicted CH_4 fluxes with treatment-specific R^2 values; dashed line indicates the 1:1 relationship. (c) Seasonal cumulative CH_4 emissions derived from observed and simulated fluxes. (d) Estimated model parameters, including maximum CH_4 production rates of fast and slow carbon pools (and), Fe half-saturation constant (), optimum temperature for CH_4 production (), temperature response width (), and carbon pool turnover rates (and).

3.4. Grain arsenic and cadmium accumulation

The accumulation of As and Cd in rice grain and husk was quantified to evaluate whether PLA-induced CH_4 mitigation was associated with food-safety trade-offs (Fig. 4). In grains, As concentrations did not differ significantly between −PLA and +PLA within either season (main: 511 ± 96 vs. 594 ± 69 μg kg^{-1}; ratoon: 622 ± 142 vs. 584 ± 181 μg kg^{-1}; all $p > 0.2$), nor between seasons for a given treatment (−PLA: $p = 0.243$; +PLA: $p = 0.915$), indicating limited treatment or seasonal effects on grain As (Fig. 4a). In husks, As concentrations were 5–10-fold higher than in grains, with within-season treatment differences remaining non-significant (main: 2859 ± 967 vs. 2639 ± 973 μg kg^{-1}; ratoon: 5543 ± 2729 vs. 6189 ± 1435 μg kg^{-1}; all $p > 0.6$). A significant seasonal increase in husk As was detected under +PLA (2639 vs. 6189 μg kg^{-1}, $p = 0.012$), but not under −PLA ($p = 0.121$) (Fig. 4b), indicating that seasonal effects outweighed treatment effects on As accumulation.

For Cd, grain concentrations showed no significant differences between −PLA and +PLA within the same season (main: 408 ± 104 vs. 404 ± 130 μg kg^{-1}; ratoon: 126 ± 62 vs. 77 ± 44 μg kg^{-1}; all $p > 0.2$) (Fig. 4c). A pronounced seasonal decline was observed regardless

of treatment, with significantly lower grain Cd in the ratoon crop than in the main crop (−PLA: 408 ± 104 vs. 126 ± 62 μg kg^{-1}, p = 0.008; +PLA: 404 ± 130 vs. 77 ± 44 μg kg^{-1}, p = 0.007). In husks, Cd concentrations were lower than in grains and did not differ significantly between treatments or seasons (main: 292 ± 184 vs. 157 ± 70 μg kg^{-1}; ratoon: 140 ± 48 vs. 134 ± 103 μg kg^{-1}; all p > 0.16) (Fig. 4d).

Across both seasons, PLA application had no significant effect on As or Cd concentrations in either grain or husk, whereas seasonal factors accounted for most of the observed variability. Grain As concentrations (511–622 μg kg^{-1} across treatments and seasons) exceeded the Chinese food safety limit for brown rice (350 μg kg^{-1}), while grain Cd concentrations (77–408 μg kg^{-1}) remained below the corresponding standard (200 μg kg^{-1}) under the sustained flooding regime used in this study.

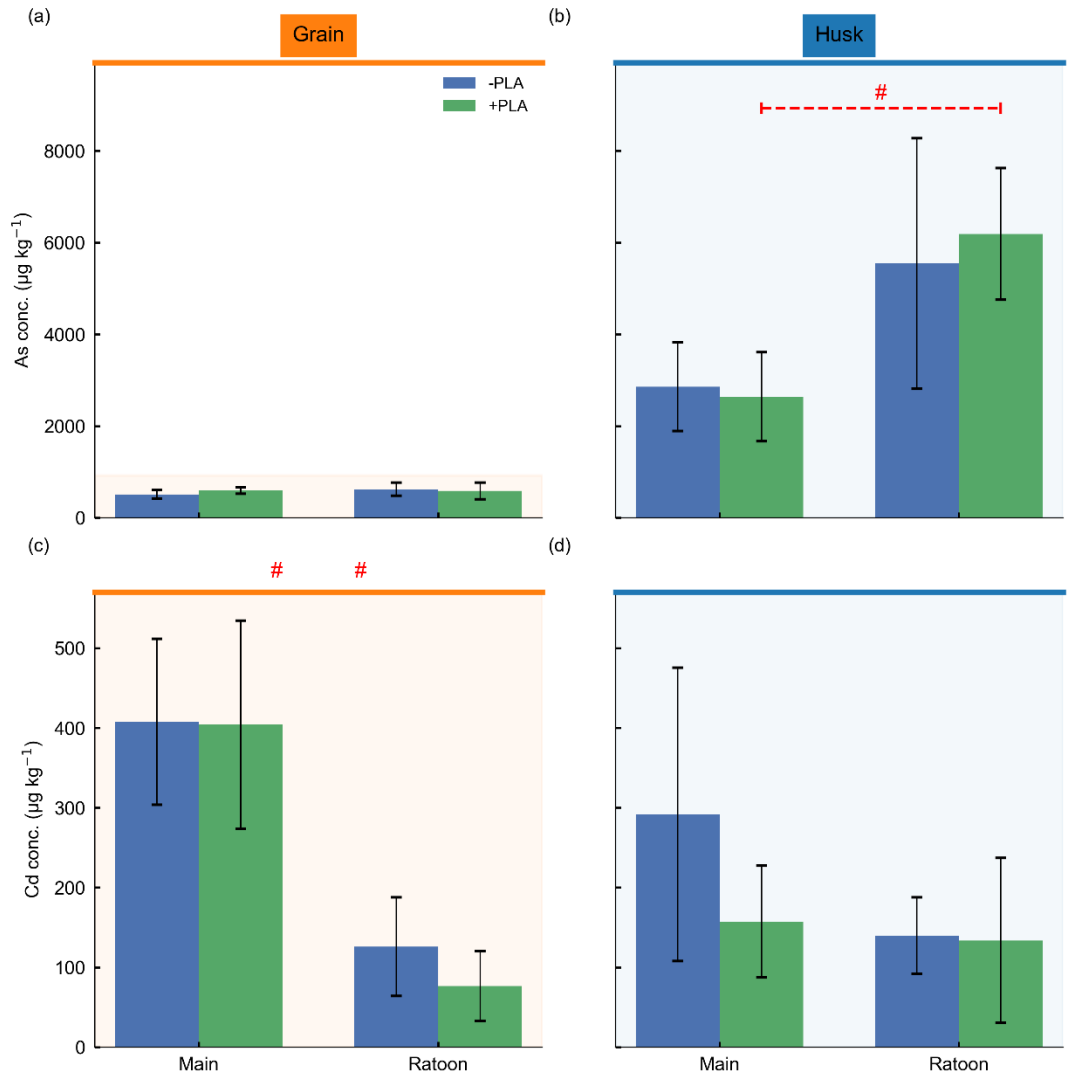

Fig. 4. Concentrations of arsenic (As) and cadmium (Cd) in rice grain and husk under −PLA and +PLA treatments during the main crop and ratoon crop seasons. Bars represent mean values with standard deviations. For each element, results are shown separately for grain (left column) and husk (right column), with the main crop and ratoon crop displayed within each panel. Background shading distinguishes grain and husk panels. Asterisks indicate statistically significant differences ($p < 0.05$) between −PLA and +PLA treatments within the same cropping season.

4. Discussion

4.1 PLA microplastics regulate CH_4 emissions through stabilized soil redox dynamics

Methane emissions in flooded rice systems are tightly coupled to soil redox dynamics, which simultaneously regulate greenhouse gas production and metal(loid) mobility [33, 38, 39]. Typically, strongly reduced conditions stimulate methanogenesis and As mobilization while suppressing Cd availability through sulfide precipitation, generating inherent trade-offs between climate mitigation and grain food safety [40]. However, PLA amendment altered this expected coupling: Despite substantial reductions in cumulative CH_4 emissions, grain metal(loid) concentrations remained unchanged (Fig. 4), indicating that PLA induced moderate and stabilized redox regulation rather than large oxidative perturbations [41, 42].

This decoupling suggests that CH_4 mitigation did not arise from overall shifts toward oxidized soil conditions but from constrained electron flow within competing anaerobic pathways. Supporting evidence is that, under flooded conditions, terminal electron-accepting processes operate hierarchically, with Fe(III) reduction thermodynamically preceding methanogenesis [15, 24]. The observed responses (i.e., lower porewater Fe/As under PLA treatment, Fig. 2, S3) therefore support a mechanism in which PLA-associated surfaces or functional groups subtly favor alternative electron sinks [15, 43], limiting methanogenic dominance while maintaining overall biogeochemical stability.

4.2 Phenological control overrides temperature sensitivity under PLA amendment

Methane emissions from flooded rice systems are inherently constrained by crop phenology through plant-mediated carbon allocation, rhizosphere development, and substrate delivery to anaerobic microbial communities [33, 38, 39], and inherent temperature dependence in extended temporal scale [44-46]. Across the growing cycle, CH_4 dynamics closely followed

crop developmental stages, indicating that ecosystem progression rather than short-term thermal variability governed emission trajectories. To disentangle these controls, we applied a phenology-constrained gray-box CH_4 model that integrates plant carbon partitioning, labile substrate turnover, temperature responses, and Fe(III)-mediated redox competition within a mass-conserving framework (Fig. 5). Given PLA's negligible biodegradation under flooded mesophilic conditions [47-49], it was parameterized as a physicochemical disturbance rather than a labile carbon source. The model robustly reproduced observed fluxes and treatment contrasts while constraining emergent ecosystem behavior, without resolving fine-scale microbial pathways (e.g., CH4MOD/DNDC gray-box approaches[45, 50]).

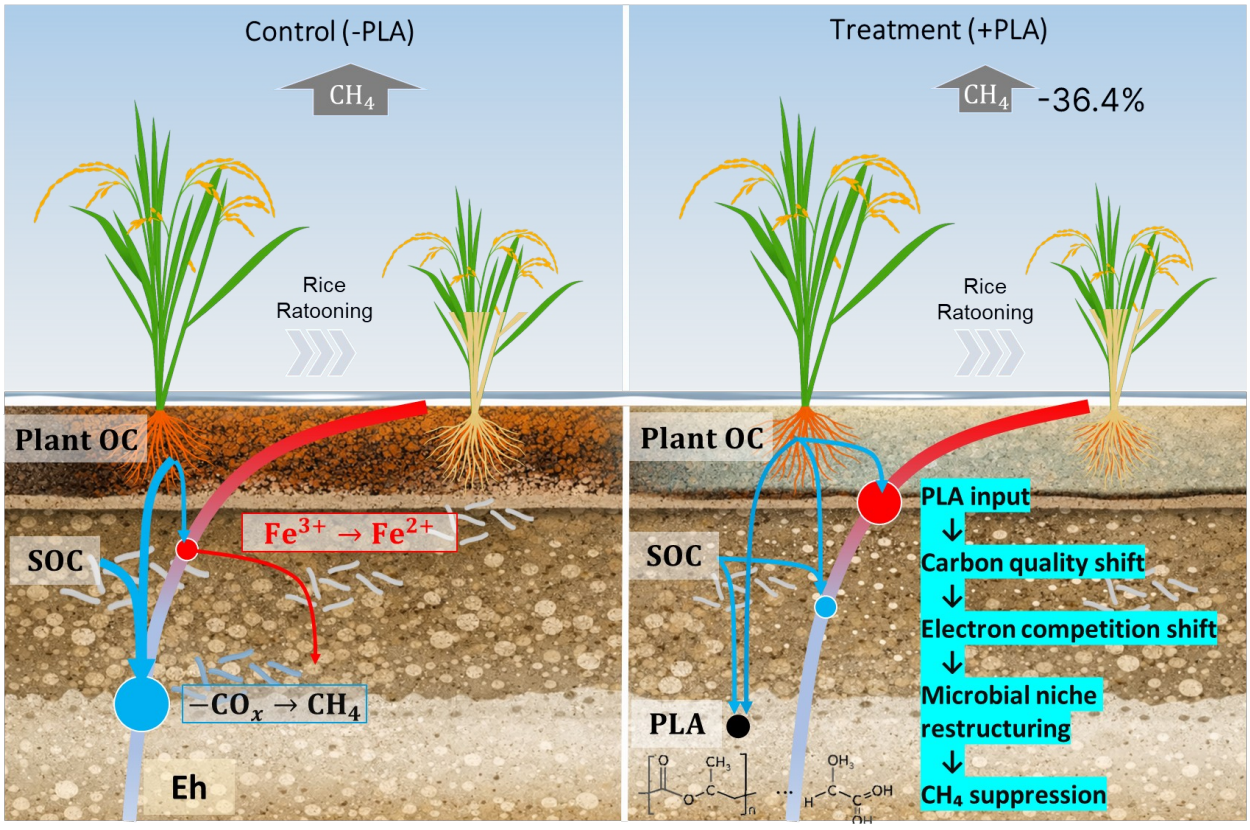

Fig. 5. Conceptual framework of PLA-mediated CH_4 suppression mechanism in ratoon rice. PLA powder introduces reactive polymer surfaces enriched with oxygen-containing groups [14, 21]. Slow PLA degradation redirects labile soil/plant carbon toward

polymer-associated microbial sinks [10], skewing the electron acceptor-donor balance away from methanogenesis toward competing anaerobic pathways (Fe(III) reduction, fermentation).

Consistent across simulations, PLA treatment reduced apparent temperature sensitivity while preserving phenological timing of emissions (Fig. 3, ref[10]), indicating strengthened biological regulation of methanogenesis. These results suggested that PLA stabilized rhizosphere redox microenvironments, limiting rapid coupling between transient carbon inputs and methanogenic response. Collectively, model–data agreement supports interpretation that modest microscale perturbations propagate through phenology-regulated plant–soil feedbacks to generate amplified ecosystem-scale reductions in CH_4 emissions.

4.3 Low-dose biodegradable materials as regulators of soil–climate feedbacks

These findings suggested a less popular idea, contrasting to the prevailing perception of biodegradable plastics solely as emerging contaminants in agricultural soils [10, 13, 14, 41, 43]. While concerns surrounding microplastic accumulation remain valid, environmentally realistic, low-dose PLA inputs may also interact with soil biogeochemical feedbacks in functionally significant ways. Rather than serving as readily degradable carbon substrates during crop growth periods, slowly degrading PLA particles appear to operate as persistent physicochemical modifiers within the soil matrix [6, 8, 9, 42]. Because pristine PLA was applied, long-term environmental aging and degradation may alter surface reactivity[10]; however, such changes are expected to influence effect magnitude rather than direction under field conditions [15, 21]. By influencing redox-mediated microbial competition without disrupting crop productivity or gas exchange balance, PLA amendment reveals an unexpected pathway linking material residues with ecosystem-scale CH_4 regulation.

4.4 Implications for carbon-neutral rice production systems

Rice cultivation represents one of the largest agricultural sources of anthropogenic CH_4 emissions globally, creating a major challenge for climate mitigation without compromising food security. This study provides the first life-cycle evidence that environmentally relevant PLA microplastic (0.01% w/w) reduces cumulative CH_4 emissions by 36.4% over 167 days of continuous flooding spanning main and ratoon rice crops. This value exceeded the 27.9% CH_4 reduction observed over 50 days in anaerobic slurry experiments amended with 1% PLA powder [15]. The observed CH_4 reduction achieved under environmentally realistic PLA exposure highlights a previously overlooked interface between biodegradable material cycles and low-carbon agricultural management. Importantly, CH_4 mitigation occurred without detectable penalties to yield performance, CO_2 exchange, or grain food safety, suggesting that moderate redox stabilization may offer a viable pathway toward synergistic climate–environment governance [16]. These results indicate that material innovations designed for waste reduction may simultaneously influence ecosystem carbon dynamics [16], expanding the conceptual scope of nature-based mitigation strategies supporting carbon-neutral food production.

4.5 Limitations and future perspectives

Although system-level indicators consistently support a redox-mediated mechanism, individual microbial pathways and electron transfer processes were inferred rather than directly quantified. Future work integrating microbial functional genomics, iron cycling measurements, and long-term field observations will be necessary to resolve mechanistic details and assess persistence across soil types and management regimes. In addition, long-term accumulation effects of biodegradable microplastics remain uncertain. Evaluating dose thresholds [16], degradation trajectories [6, 8-10], and multi-season responses [14, 51] will be critical for determining whether such materials ultimately function as transient regulators or enduring components of agricultural soil systems.

Conclusion

Across a full ratoon rice cycle, environmentally realistic PLA microplastic inputs significantly reduced CH_4 emissions without affecting crop productivity or grain safety. Methane mitigation was driven by persistent soil redox regulation rather than direct temperature forcing, resulting in reduced emission sensitivity to heat extremes. By decoupling greenhouse gas reduction from food-safety trade-offs, this study reveals an unexpected climate-regulatory function of biodegradable materials in agricultural ecosystems and suggests new opportunities for integrating waste-derived materials into carbon-neutral farming strategies.

Supplementary information

Supporting information includes 1 table and 4 figures: Table S1 Pearson correlations between ln(CH_4 flux) and environmental variables by treatment group; Fig. S1. Lagged relationships between CO_2 flux and CH_4 flux under −PLA and +PLA treatments. Fig. S2. Relationships between temperature and CO_2 flux under different plastic treatments; Fig. S3. Temporal dynamics of dissolved Fe concentration in flooded soils.

Author contributions

Sha Zhang: Conceptualization, Methodology, Investigation, Data curation, Writing – original draft, Writing – review & editing, Supervision. Qianrui Huangfu: Formal analysis, Visualization, Writing – original draft. Lu Wang: Investigation, Funding acquisition, Validation. Zheng Chen: Supervision, Funding acquisition, Writing – review & editing. Dong Zhu: Conceptualization, Funding acquisition, Supervision.

Data availability

The data that supports the findings of this study are available from the corresponding author upon reasonable request.

Funding

This work was supported by the National Science Foundation of China (Nos. 42595623 and 42477116) and the Ningbo Yongjiang Talent Project (Grant No. 2022A-163-G).

Conflict of Interests

The authors declare no conflict of interests.

References

[1] M. Saunois, A. Martinez, B. Poulter, Z. Zhang, P. Raymond, P. Regnier, J.G. Canadell, R.B. Jackson, P.K. Patra, P. Bousquet, Global Methane Budget 2000–2020, Earth System Science Data Discussions 2024 (2024) 1-147. https://doi.org/10.5194/essd-17-1873-2025.

[2] M. Nikolaisen, T. Cornulier, J. Hillier, P. Smith, F. Albanito, D. Nayak, Methane emissions from rice paddies globally: A quantitative statistical review of controlling variables and modelling of emission factors, J. Clean. Prod. 409 (2023) 137245. https://doi.org/10.1016/j.jclepro.2023.137245.

[3] Y. Huang, Q. Liu, W. Jia, C. Yan, J. Wang, Agricultural plastic mulching as a source of microplastics in the terrestrial environment, Environ. Pollut. 260 (2020) 114096. https://doi.org/10.1016/j.envpol.2020.114096.

[4] S.M. Satti, A.A. Shah, T.L. Marsh, R. Auras, Biodegradation of poly (lactic acid) in soil microcosms at ambient temperature: evaluation of natural attenuation, bio-augmentation and bio-stimulation, J. Environ. Polym. Degrad. 26(9) (2018) 3848-3857. https://doi.org/10.1007/s10924-018-1264-x.

[5] M.J. Krause, T.G. Townsend, Life-cycle assumptions of landfilled polylactic acid underpredict methane generation, Environ. Sci. Technol. Lett. 3(4) (2016) 166-169. https://doi.org/10.1021/acs.estlett.6b00068.

[6] J.J. Kolstad, E.T. Vink, B. De Wilde, L. Debeer, Assessment of anaerobic degradation of Ingeo™ polylactides under accelerated landfill conditions, Polymer Degradation and Stability, 2012, pp. 1131-1141.

[7] I.E. Napper, R.C. Thompson, Environmental deterioration of biodegradable, oxo-biodegradable, compostable, and conventional plastic carrier bags in the sea, soil, and open-air over a 3-year period, Environ. Sci. Technol. 53(9) (2019) 4775-4783. https://doi.org/10.1021/acs.est.8b06984.

[8] F. Battista, N. Frison, D. Bolzonella, Can bioplastics be treated in conventional anaerobic digesters for food waste treatment?, Environ. Technol. Innov. 22 (2021) 101393. https://doi.org/10.1016/j.eti.2021.101393.

[9] M. Olaya-Rincon, J. Serra-Rada, M. Casallas-Ojeda, J. Dosta, R. Torres, M. Martínez, S. Astals, Temperature and particle size influence on polylactic acid

anaerobic biodegradation, J. Environ. Chem. Eng. 14(2) (2026) 121618. https://doi.org/10.1016/j.jece.2026.121618.

[10] B. Lin, Q. Fan, F. Liu, L. Wang, C. Wei, B. Liu, J. Zhao, L. Zuo, Y. Xie, From biodegradation to biohazard: Polylactic acid microplastics induced rice growth inhibition in agroecosystems, J. Hazard. Mater. 496 (2025) 139420. https://doi.org/10.1016/j.jhazmat.2025.139420.

[11] H.Y. Sintim, M. Flury, Is biodegradable plastic mulch the solution to agriculture's plastic problem?, Environ. Sci. Technol. 51(3) (2017) 1068-1069. https://doi.org/10.1021/acs.est.6b06042.

[12] Y. Qi, X. Yang, A.M. Pelaez, E. Huerta Lwanga, N. Beriot, H. Gertsen, P. Garbeva, V. Geissen, Macro- and micro- plastics in soil-plant system: Effects of plastic mulch film residues on wheat (Triticum aestivum) growth, Sci. Total Environ. 645 (2018) 1048-1056. https://doi.org/10.1016/j.scitotenv.2018.07.229.

[13] Y. He, Y. Li, X. Yang, Y. Liu, H. Guo, Y. Wang, T. Zhu, Y. Tong, B.-J. Ni, Y. Liu, Biodegradable microplastics aggravate greenhouse gas emissions from urban lake sediments more severely than conventional microplastics, Water Res. 266 (2024) 122334. https://doi.org/10.1016/j.watres.2024.122334.

[14] J. Huang, Y. Feng, H. Xie, X. Liu, Q. Zhang, B. Wang, B. Xing, Biodegradable microplastics aging processes accelerated by returning straw in paddy soil, Sci. Total Environ. 945 (2024) 173930. https://doi.org/10.1016/j.scitotenv.2024.173930.

[15] L. Wang, X. Lu, Y. Yao, X. Liu, T. Ge, Y. Luo, H. Jia, L. Van Zwieten, G. Guggenberger, Mechanisms associated with lower methane emissions from paddy soil by aged polylactic acid microplastics, Environ. Sci. Technol. 59(50) (2025) 27378-27392. https://doi.org/10.1021/acs.est.5c11590.

[16] M. Xiao, M. Shahbaz, Y. Liang, J. Yang, S. Wang, D.R. Chadwicka, D. Jones, J. Chen, T. Ge, Effect of microplastics on organic matter decomposition in paddy soil amended with crop residues and labile C: A three-source-partitioning study, J. Hazard. Mater. 416 (2021) 126221. https://doi.org/10.1016/j.jhazmat.2021.126221.

[17] J. Cheng, J. Hua, T. Kang, B. Meng, L. Yue, H. Dong, H. Li, J. Zhou, Nanoscale zero-valent iron improved lactic acid degradation to produce methane through anaerobic digestion, Bioresour. Technol. 317 (2020) 124013. https://doi.org/10.1016/j.biortech.2020.124013.

[18] A. Chamas, H. Moon, J. Zheng, Y. Qiu, T. Tabassum, J.H. Jang, M. Abu-Omar, S.L. Scott, S. Suh, Degradation rates of plastics in the environment, ACS Sustain. Chem. Eng. 8(9) (2020) 3494-3511. https://doi.org/10.1021/acssuschemeng.9b06635.

[19] T. Fumoto, Process-based modeling of methane emissions from rice fields, Bulletin of the NARO, Agro-Environmental Sciences (38) (2017). https://www.naro.go.jp/publicity_report/publication/files/niaes_report38-2.pdf.

[20] X. Xiao, M.E. Hodson, J.B. Sallach, Biodegradable microplastics adsorb more Cd than conventional microplastic and biofilms enhance their adsorption, Chemosphere 371 (2025) 144062. https://doi.org/10.1016/j.chemosphere.2025.144062.

[21] C. Lei, M. Chengkai, Y. Shanning, P. Xianjuan, L. Huanhuan, C. Xiangyu, S. Haiyang, W. Minghong, Comparison of aging behavior and adsorption processes of biodegradable and conventional microplastics, Chem. Eng. J. 502 (2024) 157915. https://doi.org/10.1016/j.cej.2024.157915.

[22] O. Sivan, S.S. Shusta, D.L. Valentine, Methanogens rapidly transition from methane production to iron reduction, Geobiology 14(2) (2016) 190-203. https://doi.org/10.1111/gbi.12172.

[23] J. Zheng, T. RoyChowdhury, Z. Yang, B. Gu, S.D. Wullschleger, D.E. Graham, Impacts of temperature and soil characteristics on methane production and oxidation in Arctic tundra, Biogeosciences 15(21) (2018) 6621-6635. https://doi.org/10.5194/bg-15-6621-2018.

[24] T. Borch, R. Kretzschmar, A. Kappler, P.V. Cappellen, M. Ginder-Vogel, A. Voegelin, K. Campbell, Biogeochemical redox processes and their impact on contaminant dynamics, Environ. Sci. Technol. 44(1) (2010) 15-23. https://doi.org/10.1021/es9026248.

[25] H.-C. Tseng, N. Fujimoto, A. Ohnishi, Biodegradability and methane fermentability of polylactic acid by thermophilic methane fermentation, Bioresour. Technol. Rep. 8 (2019) 100327. https://doi.org/10.1016/j.biteb.2019.100327.

[26] Q. Huangfu, S. Zhang, Y. Guo, L. Wang, Z. Chen, S. Du, Elevated soil temperatures during a heatwave year do not necessarily increase metal(loid) mobilization or accumulation across two harvests of semi-perennial rice: evidence from mesocosm experiments, Environ. Biogeochem. Process. 1(1) (2025). https://doi.org/10.48130/ebp-0025-0017.

[27] E.C.f. Standardization, Packaging - Requirements for packaging recoverable through composting and biodegradation - Test scheme and evaluation criteria for

the final acceptance of packaging, CEN (European Committee for Standardization), Brussels, 2000.

[28] J.J. Kolstad, E.T.H. Vink, B. De Wilde, L. Debeer, Assessment of anaerobic degradation of Ingeo™ polylactides under accelerated landfill conditions, Polym. Degrad. Stab. 97(7) (2012) 1131-1141. http/doi.org/10.1016/j.polymdegradstab.2012.04.003.

[29] M. Ueyama, R. Takeuchi, Y. Takahashi, R. Ide, M. Ataka, Y. Kosugi, K. Takahashi, N. Saigusa, Methane uptake in a temperate forest soil using continuous closed-chamber measurements, Agric. For. Meteorol. 213 (2015) 1-9. https://doi.org/10.1016/j.agrformet.2015.05.004.

[30] S. Zhang, Q. Huangfu, D. Zhu, Z. Chen, Floating iron biofilms as hidden barriers to methane emissions in wetlands, Innov. Geosci. 3(4) (2025) 100161-100161. https://doi.org/10.59717/j.xinn-geo.2025.100161.

[31] S. Zhang, J. Song, L. Wu, S. Du, L. Wang, D. Zhu, Z. Chen, Soil microdialysis as a tool to simulate rhizosphere dynamics and estimate metal(loid) uptake in radish (Raphanus sativus L.), Plant Soil (2025). https://doi.org/10.1007/s11104-025-07958-7.

[32] S. Zhang, Z. Yuan, Y. Cai, H. Liu, Z. Liu, Z. Chen, Dissolved solute sampling across an oxic-anoxic soil-water interface using microdialysis profilers, JOVE (193) (2023) e64358. https://doi.org/10.3791/64358.

[33] G. McNicol, E. Fluet-Chouinard, Z. Ouyang, S. Knox, Z. Zhang, T. Aalto, S. Bansal, K.-Y. Chang, M. Chen, K. Delwiche, S. Feron, M. Goeckede, J. Liu, A. Malhotra, J.R. Melton, W. Riley, R. Vargas, K. Yuan, Q. Ying, Q. Zhu, P. Alekseychik, M. Aurela, D.P. Billesbach, D.I. Campbell, J. Chen, H. Chu, A.R. Desai, E. Euskirchen, J. Goodrich, T. Griffis, M. Helbig, T. Hirano, H. Iwata, G. Jurasinski, J. King, F. Koebsch, R. Kolka, K. Krauss, A. Lohila, I. Mammarella, M. Nilson, A. Noormets, W. Oechel, M. Peichl, T. Sachs, A. Sakabe, C. Schulze, O. Sonnentag, R.C. Sullivan, E.-S. Tuittila, M. Ueyama, T. Vesala, E. Ward, C. Wille, G.X. Wong, D. Zona, L. Windham-Myers, B. Poulter, R.B. Jackson, Upscaling wetland methane emissions from the fluxnet-ch4 eddy covariance network (upch4 v1.0): model development, network assessment, and budget comparison, AGU Advances 4(5) (2023) e2023AV000956. https://doi.org/10.1029/2023AV000956.

[34] S. van de Velde, F.J.R. Meysman, The influence of bioturbation on iron and sulphur cycling in marine sediments: A model analysis, Aquat. Geochem. 22(5) (2016) 469-504. https://doi.org/10.1007/s10498-016-9301-7.

[35] J.B. van Hulzen, R. Segers, P.M. van Bodegom, P.A. Leffelaar, Temperature effects on soil methane production: an explanation for observed variability, Soil Biol. Biochem. 31(14) (1999) 1919-1929. https://doi.org/10.1016/S0038-0717(99)00109-1.

[36] G. Yvon-Durocher, A.P. Allen, D. Bastviken, R. Conrad, C. Gudasz, A. St-Pierre, N. Thanh-Duc, P.A. del Giorgio, Methane fluxes show consistent temperature dependence across microbial to ecosystem scales, Nature 507(7493) (2014) 488-491. https://doi.org/10.1038/nature13164.

[37] B. Lee, H. Kwon, P. Zhao, J. Tenhunen, Improved gross primary production estimation in rice fields through integrated multi-scale methodologies, Plant Environ. Interact. 4(3) (2023) 163-174. https://doi.org/10.1002/pei3.10109.

[38] J. Li, H. Chen, A. Ding, X. Chi, W. Ju, Y. Zhang, P. Ciais, W. Yuan, S. Peng, Z. Ma, G. Yu, J.M. Chen, Temporal variations of δ(13)C-CH(4) in rice paddies dominated by the plant-mediated pathway, iScience 28(7) (2025) 112886. https://doi.org/10.1016/j.isci.2025.112886.

[39] S. Guan, Z. Qi, S. Li, S. Du, D. Xu, Effects of rice root development and rhizosphere soil on methane emission in paddy fields, Plants (Basel) 13(22) (2024). https://doi.org/10.3390/plants13223223.

[40] N. Yamaguchi, T. Nakamura, D. Dong, Y. Takahashi, S. Amachi, T. Makino, Arsenic release from flooded paddy soils is influenced by speciation, Eh, pH, and iron dissolution, Chemosphere 83(7) (2011) 925-932. https://doi.org/10.1016/j.chemosphere.2011.02.044.

[41] R. Liu, J. Liang, Y. Yang, H. Jiang, X. Tian, Effect of polylactic acid microplastics on soil properties, soil microbials and plant growth, Chemosphere 329 (2023) 138504. https://doi.org/10.1016/j.chemosphere.2023.138504.

[42] L. Chen, H. Huang, L. Han, L. Chao, X. Zhang, B. Liu, C. Luo, W. Mo, Y. Cai, Z. Yang, Effects of polylactic acid microplastics on dissolved organic matter across soil types: Insights into molecular composition, J. Hazard. Mater. 488 (2025) 137356. https://doi.org/10.1016/j.jhazmat.2025.137356.

[43] T. Bandara, A. Franks, G. Clark, C. Tang, Fate of nano/microplastics and associated toxic pollutants in paddy ecosystems: Current knowledge and future

perspectives, Earth Critical Zone 1(1) (2024) 100013. https://doi.org/10.1016/j.ecz.2024.100013.

[44] X. Liu, X. Dai, F. Yang, S. Meng, H. Wang, CH_4 emissions from a double-cropping rice field in subtropical China over seven years, Agric. For. Meteorol. 339 (2023) 109578. https://doi.org/10.1016/j.agrformet.2023.109578.

[45] Q. Hu, J. Li, H. Xie, Y. Huang, J.G. Canadell, W. Yuan, J. Wang, W. Zhang, L. Yu, S. Li, X. Lu, T. Li, Z. Qin, Global methane emissions from rice paddies: CH4MOD model development and application, iScience 27(11) (2024) 111237. https://doi.org/10.1016/j.isci.2024.111237.

[46] R. Conrad, Control of microbial methane production in wetland rice fields, Nutrient Cycling in Agroecosystems 64(1) (2002) 59-69. https://doi.org/10.1023/A:1021178713988.

[47] H. Zang, J. Zhou, M.R. Marshall, D.R. Chadwick, Y. Wen, D.L. Jones, Microplastics in the agroecosystem: Are they an emerging threat to the plant-soil system?, Soil Biol. Biochem. 148 (2020) 107926. https://doi.org/10.1016/j.soilbio.2020.107926.

[48] Y.M. Lozano, T. Lehnert, L.T. Linck, A. Lehmann, M.C. Rillig, Microplastic shape, polymer type, and concentration affect soil properties and plant biomass, Front. Plant Sci. 12 (2021) 169.

[49] M. Mohan, Z.U. Abedien, P. Kaparaju, Thermophilic anaerobic digestion of polylactic acid, polyethylene and polypropylene microplastics: effect of inoculum-substrate ratio and microbiome, Biodegradation 36(5) (2025) 95. https://doi.org/10.1007/s10532-025-10186-6.

[50] K.W. Proctor, N. Chatterjee, C. Jones, C. Hill, The denitrification-decomposition (DNDC) model, in: G. Hoogenboom (Ed.), Current crop models: State-of-the-art and future developments, Burleigh Dodds Science Publishing Limited, Cambridge, UK, 2025, pp. 223-252. https://doi.org/10.19103/AS.2025.0155.09.

[51] S. Lai, C. Fan, P. Yang, Y. Fang, L. Zhang, M. Jian, G. Dai, J. Liu, H. Yang, L. Shen, Effects of different microplastics on the physicochemical properties and microbial diversity of rice rhizosphere soil, Front. Microbiol. 15 (2025) 1513890. https://doi.org/10.3389/fmicb.2024.1513890.